Telecommunications, Networks, Electronics, and Computer Techonologies

Vol.6 (1), 2026, 7-17

JURNAL UPI

TELNECT

Journal homepage: http://ejournal-purwakarta.upi.edu/telnect/

Effects of DC-Link Capacitance on Output Voltage Quality and Power Delivery in a Three-Phase Diode Rectifier

Elysa Nensy Irawan[1,2*]

[1]Department of Mechatronics and Artificial Intelligence, Universitas Pendidikan Indonesia, Indonesia
[2]Power System Laboratory, Shibaura Institute of Technology, Japan

*Corresponding Author: E-mail: elysanensy@upi.edu

ABSTRACTS

This study investigates the effects of DC-link capacitance on output voltage quality and load power delivery in a three-phase diode rectifier circuit. A MATLAB/Simulink model using Simscape Electrical was developed, consisting of a balanced three-phase AC source, a diode bridge rectifier, a DC-link capacitor with equivalent series resistance, and a 20 Ω resistive load. Four capacitance values, namely 470 µF, 1000 µF, 2200 µF, and 22000 µF, were evaluated under identical operating conditions. The DC-link voltage and load current were recorded to analyze the start-up response, steady-state voltage ripple, average DC-link voltage, average load power, and power fluctuation. The results show that increasing capacitance substantially improved voltage quality. The peak-to-peak voltage ripple decreased from 3.75 V at 470 µF to 0.13 V at 22000 µF, while the ripple percentage decreased from 12.75% to 0.42%. The average DC-link voltage increased from 29.39 V to 31.25 V. In addition, the average load power increased from 43.25 W to 48.83 W, whereas the peak-to-peak power fluctuation decreased from 11.28 W to 0.41 W. The results indicate that larger DC-link capacitance mainly improves output-voltage and load-power stability, while the improvement in average voltage and power becomes smaller at very high capacitance values.

ARTICLEINFO

Article History:
Received 16 June 2026
Revised 25 June 2026
Accepted 26 June 2026
Available online 30 June 2026

Keyword:
Capacitance, MATLAB/Simulink, power, ripple, voltage

1. INTRODUCTION

AC–DC conversion is an essential function in many electrical and electronic systems because a large number of loads, control circuits, and power electronic devices require a stable DC supply [1]. Three-phase diode rectifiers are commonly used for this purpose due to their simple structure, low cost, high reliability, and ability to provide a higher average DC output than single-phase rectifiers [2]. Despite these advantages, the output voltage produced by a three-phase rectifier is not perfectly constant [3]. The rectification process generates periodic voltage fluctuations, commonly referred to as DC-link voltage ripple.

Voltage ripple is an important issue because it affects the quality and stability of the DC supply [4]. When the ripple level is high, the output voltage may vary significantly over time, which can cause undesirable fluctuations in load current and delivered power [5]. In practical applications, excessive ripple may also increase electrical stress on downstream circuits, reduce the performance of sensitive electronic loads, and affect the reliability of power conversion systems [6]. Therefore, smoothing the rectified voltage is an important consideration in DC power supply design.

A DC-link capacitor is typically connected across the output terminals of a rectifier to reduce voltage ripple [7]. The capacitor acts as an energy-storage component that absorbs energy when the rectified voltage reaches a high level and supplies energy to the load when the rectified voltage decreases [8]. Through this charging and discharging process, the capacitor helps maintain the DC-link voltage at a more stable level [9]. As a result, the capacitance value strongly influences the electrical behavior of the rectifier output.

In general, a small DC-link capacitor discharges more rapidly between rectifier charging intervals [10]. This condition leads to a larger voltage drop and more visible ripple in the DC-link waveform. Conversely, a larger capacitor can store more electrical energy and maintain the output voltage closer to its peak level [11]. Therefore, increasing capacitance generally improves voltage smoothing and reduces the amplitude of voltage ripple.

However, selecting a large capacitor is not always the best solution. Larger capacitors require more physical space and may increase the overall cost of the circuit [12]. In addition, when a circuit is energized, a large capacitor can initially draw a high charging current [13]. This inrush current may impose additional stress on the rectifier diodes, source components, wires, protection devices, and the capacitor itself. Consequently, DC-link capacitor selection involves an important trade-off between voltage ripple reduction and electrical stress during circuit operation.

The capacitance value also influences transient behaviour [14]. When the input source or load condition changes, the DC-link capacitor responds by storing or releasing energy to reduce voltage variation [15]. A small capacitor may respond quickly but may not provide sufficient voltage support during transient conditions. In contrast, a large capacitor can maintain the voltage more effectively, but it may require a longer charging period and may increase the magnitude of the initial charging current [16]. These characteristics indicate that capacitance affects both steady-state voltage quality and dynamic circuit performance.

In many power-electronic studies, DC-link capacitors are discussed as part of complex systems such as motor drives [17], inverters [18], renewable-energy interfaces [19], active power filters [20], and switched-mode converters [21]. In these systems, the behaviour of the capacitor is influenced by additional factors, including control strategies, switching frequency [22], modulation techniques, and multiple power-conversion stages [23]. Although these studies are important, the basic relationship between DC-link capacitance and rectifier output characteristics can become difficult to observe independently.

A focused analysis of a three-phase diode rectifier circuit is therefore useful for understanding the fundamental role of DC-link capacitance. Such an analysis can clarify how changes in capacitance influence DC-link voltage stability, ripple magnitude, charging behaviour, transient response, and electrical stress. This fundamental understanding is important because the DC-link capacitor is one of the most frequently used passive components in power conversion circuits. This study focuses on the effect of different DC-link capacitance values on the output characteristics of a three-phase rectifier circuit. The objective is to identify the trade-off between voltage smoothing performance and practical electrical considerations.

2. MATERIALS AND METHODS

This section describes the simulation methodology used to evaluate the effects of DC-link capacitance on output voltage quality and load power delivery in a three-phase diode rectifier circuit. The circuit model was developed in MATLAB/Simulink using the Simscape Electrical library.

2.1 Simulation Framework

Figure 1 illustrates the overall Simulink-based circuit configuration used in this study. The model was developed in MATLAB/Simulink using the Simscape Electrical library and consisted of four main sections: a balanced three-phase AC source, a three-phase diode bridge rectifier, a DC-link capacitor branch, and a resistive load.

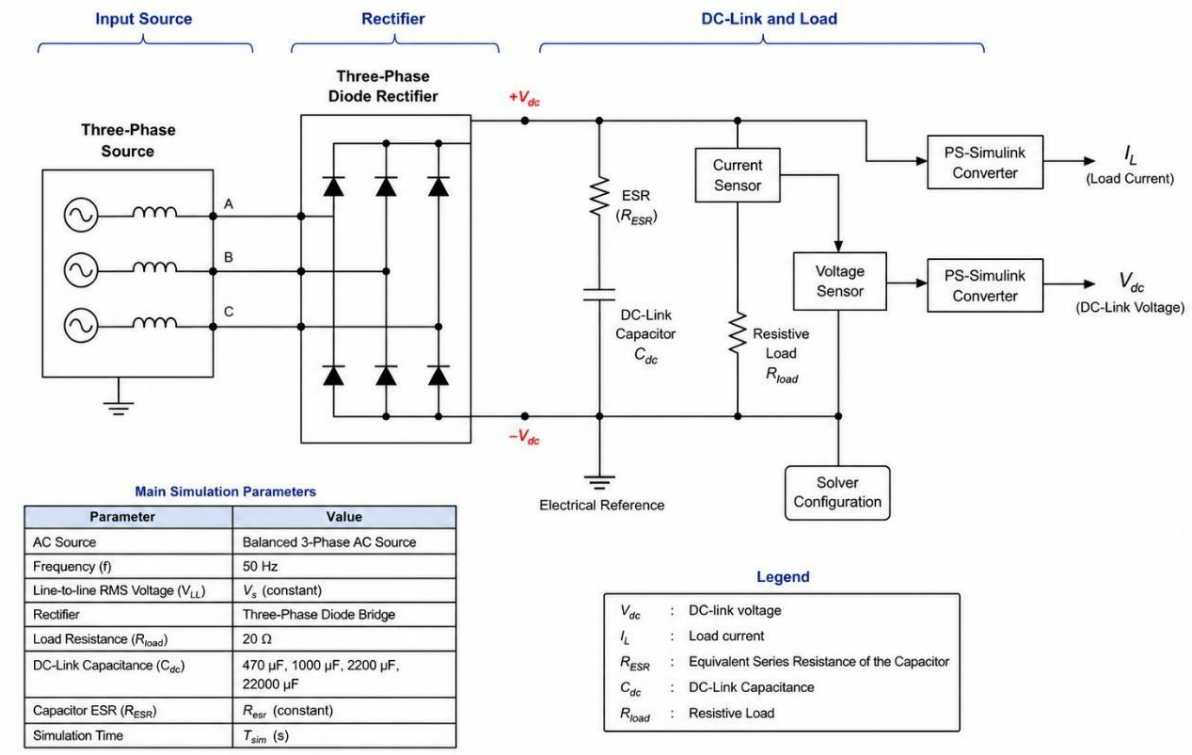

Parameter	Value
AC Source	Balanced 3-Phase AC Source
Frequency (f)	50 Hz
Line-to-line RMS Voltage (V_{LL})	V_s (constant)
Rectifier	Three-Phase Diode Bridge
Load Resistance (R_{load})	20 Ω
DC-Link Capacitance (C_{dc})	470 µF, 1000 µF, 2200 µF, 22000 µF
Capacitor ESR (R_{ESR})	R_{esr} (constant)
Simulation Time	T_{sim} (s)

Figure 1. Simulink-based configuration of the three-phase diode rectifier circuit with a DC-link capacitor and resistive load.

The balanced three-phase voltage source supplied AC power to the input terminals of the diode bridge rectifier. The source frequency was maintained at 50 Hz throughout the simulations. The rectifier converted the three-phase AC input into an unregulated DC output. Because the three-phase diode bridge rectifier produces a six-pulse rectified waveform, the resulting DC output contained periodic voltage ripple.

A DC-link capacitor branch was connected across the rectifier output and in parallel with the resistive load. The capacitor absorbed energy during high-voltage intervals of the rectified waveform and released stored energy when the rectified voltage decreased. This charging and discharging process influenced the DC-link voltage profile, particularly the voltage ripple and the average DC-link voltage.

The circuit configuration was intentionally simplified by excluding additional power-conversion stages, control systems, generators, and renewable-energy sources. This approach allowed the analysis to focus specifically on the electrical behaviour of the rectifier output and the effect of DC-link capacitance. Consequently, variations in the DC-link voltage characteristics could be attributed primarily to changes in the capacitance value.

2.2 Simulation Scenario

The simulations were organized into four capacitance cases under identical source and load conditions as shown in Table 1. The purpose of this approach was to isolate the influence of DC-link capacitance on the electrical behavior of the three-phase diode rectifier circuit. At the beginning of each simulation, the three-phase AC source was energized at $(t = 0)$ s while the initial voltage of the DC-link capacitor was set to 0 V. This initial condition allowed the capacitor charging process and the associated inrush current to be observed. The balanced three-phase source voltage, source frequency, rectifier configuration, capacitor ESR, and load resistance were maintained constant in all cases.

The simulation process was divided into two observation intervals. The first interval corresponded to the start-up transient period, during which the DC-link capacitor was charged from its initial voltage.

This interval was used to observe the voltage rise, capacitor charging behaviour and peak inrush current. The second interval corresponded to the steady-state operating period, during which the DC-link voltage waveform, voltage ripple, load current, and load power were evaluated.

The transient response was evaluated from the beginning of the simulation until the DC-link voltage reached a stable level. The steady-state analysis was conducted during the final part of the simulation, after the initial charging transient had decayed. The same steady-state observation window was applied to all cases to maintain consistency in the comparison.

TABLE 1. SIMULATION SCENARIO

Scenario	Capacitance value	Operating condition
S1	470 μF	Low-capacitance
S2	1000μF	Medium-capacitance
S3	2200μ F	High-capacitance
S4	22000μF	Very-high-capacitance

2.3 Data Analysis

The simulation outputs were exported from Simulink to the MATLAB workspace for time-domain analysis. The primary signal analyzed in this study was the DC-link voltage measured across the output terminals of the three-phase diode rectifier. The analysis was divided into two operating periods: the start-up transient period and the steady-state period. The start-up transient period was used to evaluate the initial charging behaviour of the DC-link capacitor, whereas the steady-state period was used to evaluate voltage ripple and the average DC-link voltage.

2.3.1 Start-Up Transient

The start-up transient analysis was conducted from the beginning of the simulation, when the three-phase AC source was energized and the initial capacitor voltage was set to 0 V. During this interval, the DC-link capacitor was charged through the diode bridge rectifier until the output voltage approached a stable operating level. The DC-link voltage rise was observed for each capacitance value to compare the charging response. The analysis focused on the time required for the DC-link voltage to reach and maintain a stable level. A larger capacitor was expected to provide greater energy-storage capability; however, it could also require a longer charging period before reaching steady-state operation. The start-up results were presented using DC-link voltage-versus-time waveforms from the beginning of the simulation. The comparison was used to identify differences in voltage rise characteristics among the low-, medium-, high-, and very-high-capacitance conditions.

2.3.2 Voltage Ripple

Voltage ripple analysis was performed during the steady-state operating period after the initial charging transient had decayed. To ensure a consistent comparison, the final 0.10 s of the 3 s simulation interval, from 2.90 s to 3.00 s, was selected as the steady-state observation window for all capacitance cases. The DC-link voltage waveform was examined within this interval to determine the maximum and minimum voltage levels. The difference between these values was used to represent the peak-to-peak voltage ripple. Ripple percentage was also evaluated to express the voltage variation relative to the average DC-link voltage.

A zoomed waveform over the final 20 ms of the simulation was used to clearly show the repetitive capacitor charging and discharging behaviour between successive rectifier conduction intervals. The ripple analysis focused on the reduction in voltage fluctuation as the DC-link capacitance increased. Table 2 shows ripple-related variables were recorded for each capacitance case.

TABLE 2. VARIABLES DESCRIPTION

Variable	Description
Maximum DC-link voltage	Highest voltage during the steady-state observation window
Minimum DC-link voltage	Lowest voltage during the steady-state observation window
Peak-to-peak ripple voltage	Difference between the maximum and minimum DC-link voltages
Ripple percentage	Relative magnitude of voltage ripple with respect to the average DC-link voltage

2.3.3 Average DC-Link Voltage

The average DC-link voltage was calculated from the DC-link voltage samples within the same steady-state observation window. This metric represents the average voltage supplied by the rectifier circuit after the capacitor filtering effect had been established. The average DC-link voltage was compared across the four capacitance cases to determine whether an increase in capacitance not only

reduced voltage ripple but also improved the mean output voltage. A larger capacitance was expected to maintain the DC-link voltage closer to the peak value of the rectified waveform because it could retain stored energy for a longer interval between capacitor charging periods. The analysis considered the relationship between capacitance, average DC-link voltage, and voltage ripple. It examined whether the improvement in average voltage remained substantial when the capacitance was increased from 2200 µF to 22000 µF.

2.3.4 Load Power Delivery

Load power delivery was evaluated to examine how DC-link capacitance affected the electrical power supplied to the resistive load. A current sensor was connected in series with the load resistor, while a voltage sensor was connected across the DC-link terminals. The measured load-current and DC-link-voltage signals were transferred to the Simulink workspace for post-processing. The instantaneous load power was calculated by multiplying the DC-link voltage and load current at each time instant as shown in Equation (1).

$$P_{load}(t) = V_{DC}(t) \cdot I_{load}(t) \tag{1}$$

where $P_{load}(t)$ is the instantaneous load power, $V_{DC}(t)$ is the DC-link voltage [V], and $I_{load}(t)$ is the current flowing through the resistive load [A].

The load-power characteristics were evaluated during the steady-state interval to exclude the initial capacitor-charging transient. For each capacitance case, the analysis included the average load current, average load power, maximum load power, minimum load power, and peak-to-peak power fluctuation. The average load power was calculated over the selected steady-state interval as Equation 2,

$$P_{avg} = \frac{1}{T_{ss}} \int_{t1}^{t2} P_{load}(t)\ \mathrm{dt} \tag{2}$$

where $t1$ and $t2$ represent the start and end of the steady-state observation interval, and $T_{ss} = t1\text{-}t2$. This analysis was performed for all DC-link capacitance values to compare the effect of capacitance on the average power delivered to the load and the stability of the delivered power.

3. RESULTS AND DISCUSSION

This section presents the simulation results obtained for the four DC-link capacitance values of 470 µF, 1000 µF, 2200 µF, and 22000 µF. The analysis focuses on the effect of DC-link capacitance on the start-up voltage response, steady-state voltage quality, and load power delivery in the three-phase diode rectifier circuit.

3.1 Start-Up Transient Analysis

Figure 2 shows the DC-link voltage response during the first 50 ms after the three-phase source was energized for four DC-link capacitance values: 470 µF, 1000 µF, 2200 µF, and 22000 µF. In all cases, the DC-link voltage increased rapidly from 0 V to approximately 30 V, indicating that the capacitor was charged shortly after the rectifier started operating. After the initial charging process, the voltage waveform exhibited periodic fluctuations caused by the six-pulse output of the three-phase diode rectifier.

The smallest capacitance, 470 µF, produced the largest voltage variation. Its waveform showed pronounced voltage drops between successive charging intervals, with the DC-link voltage decreasing to approximately 27–28 V before being recharged near the next rectified-voltage peak. This behaviour indicates that the stored energy in the 470 µF capacitor was insufficient to maintain the load voltage effectively during the interval between rectifier conduction periods.

Increasing the capacitance to 1000 µF reduced the depth of the voltage drops. Although periodic ripple was still clearly visible, the DC-link voltage remained closer to the upper voltage level than in the 470 µF case. A further increase to 2200 µF improved the voltage smoothing effect, producing a more stable DC-link voltage waveform with smaller fluctuations.

The 22000 µF capacitor provided the smoothest voltage response among the tested cases. Its waveform remained close to the maximum DC-link voltage for most of the observation interval, indicating that the larger capacitor was able to supply stored energy to the resistive load more effectively

during periods when the rectified voltage decreased. Consequently, the voltage ripple was substantially reduced.

These results confirm that increasing the DC-link capacitance improves the short-term voltage-holding capability of the rectifier output. However, the waveform comparison alone is insufficient to quantify the improvement. Therefore, the subsequent analysis evaluates the average DC-link voltage, maximum and minimum voltage, peak-to-peak ripple voltage, and ripple percentage during the steady-state interval.

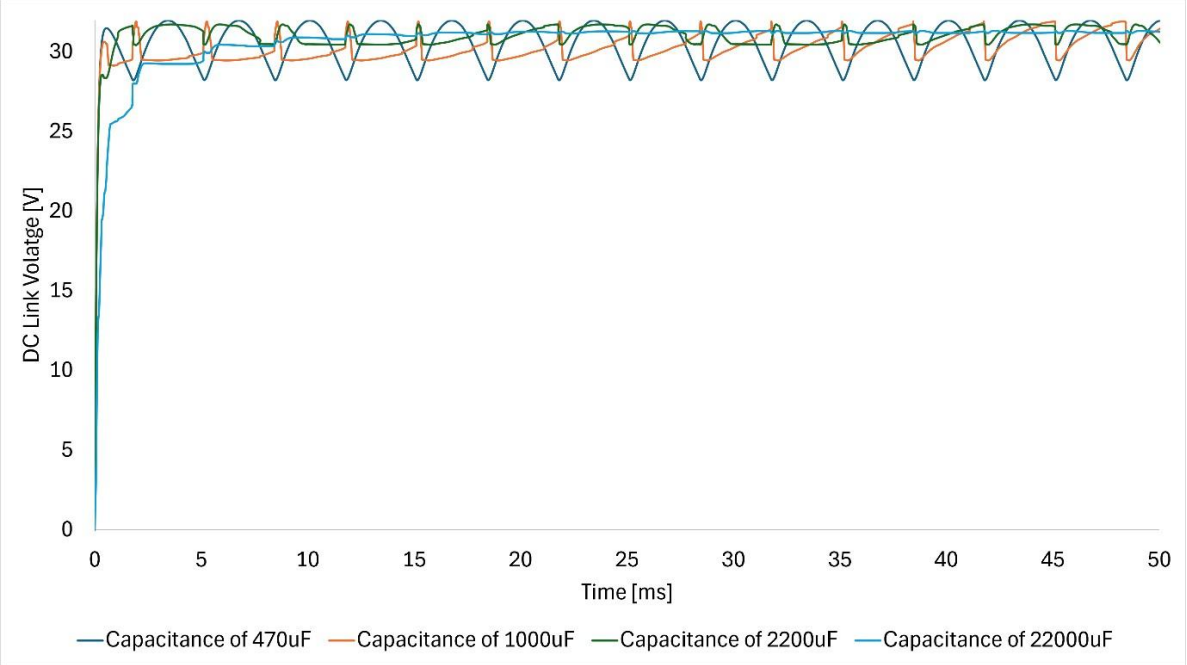

Figure 2. DC-link voltage responses for different capacitance values during the first 50 ms after source energization.

3.2 Voltage Ripple Analysis

Figure 3 presents the steady-state DC-link voltage waveforms for the four evaluated capacitance values over the interval from 9.98 s to 9.99 s. The corresponding quantitative results are summarized in Table 3. The 470 µF case exhibited the largest voltage variation among all cases. The DC-link voltage ranged from 28.22 V to 31.97 V, resulting in a peak-to-peak ripple of 3.75 V and a ripple percentage of 12.75%. Its average DC-link voltage was 29.39 V. The waveform shows substantial voltage drops between consecutive charging peaks. When the capacitance was increased to 1000 µF, the average DC-link voltage increased to 30.46 V. The minimum voltage increased to 29.47 V, while the peak-to-peak ripple decreased to 2.45 V. Consequently, the ripple percentage decreased to 8.03%. Compared with the 470 µF case, the 1000 µF capacitor reduced the peak-to-peak ripple by approximately 34.7%. Further improvement was obtained with the 2200 µF capacitor. The average DC-link voltage increased to 31.03 V, while the voltage varied between 30.46 V and 31.73 V. The peak-to-peak ripple was reduced to 1.27 V, corresponding to a ripple percentage of 4.09%. This represents a ripple reduction of approximately 66.1% relative to the 470 µF case. The 22000 µF case produced the most stable DC-link voltage waveform. The average voltage was 31.25 V, while the maximum and minimum values were 31.32 V and 31.19 V, respectively. The resulting peak-to-peak ripple was only 0.13 V, and the ripple percentage was 0.42%. Compared with the 470 µF case, the peak-to-peak ripple was reduced by approximately 96.5%.

Overall, the results demonstrate that increasing the DC-link capacitance substantially improves output voltage quality by reducing voltage ripple and increasing the minimum DC-link voltage. The average DC-link voltage increased from 29.39 V at 470 µF to 31.25 V at 22000 µF. However, the increase in average voltage was smaller than the reduction in ripple. For example, increasing the capacitance from 2200 µF to 22000 µF increased the average voltage by only 0.22 V, whereas the ripple percentage decreased from 4.09% to 0.42%. Therefore, the main benefit of increasing DC-link capacitance in this rectifier circuit is improved voltage stability rather than a large increase in average output voltage. The 22000 µF capacitor achieved the best voltage quality among the evaluated cases, while the 2200 µF case already provided a considerable reduction in ripple with an average DC-link voltage above 31 V.

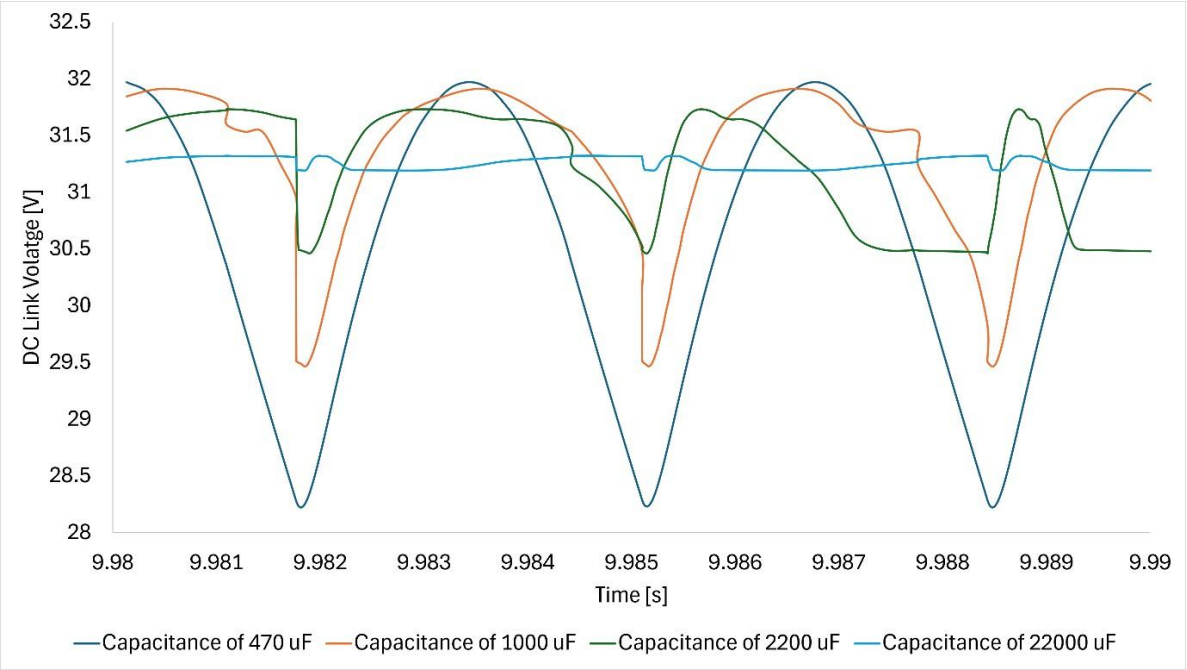

Figure 3. Steady-state DC-link voltage waveforms for different DC-link capacitance values

TABLE 4. STEADY-STATE DC-LINK VOLTAGE AND RIPPLE CHARACTERISTICS FOR DIFFERENT CAPACITANCE VALUES

Average DC Link Voltage [V]	Maximum DC Link Voltage [V]	Minimum DC Link Voltage [V]	Ripple Peak to Peak [V]	Ripple Percentage [%]
29.39	31.97	28.22	3.75	12.75
30.46	31.91	29.47	2.45	8.03
31.03	31.73	30.46	1.27	4.09
31.25	31.32	31.19	0.13	0.42

3.3 Average DC-Link Voltage

Figure 4 presents the DC-link voltage waveforms during the steady-state interval from 9.90 s to 9.95 s for the four evaluated capacitance values. The corresponding average DC-link voltages were calculated from the steady-state data, as summarized in Table 5.

The 470 µF case produced the lowest average DC-link voltage, with a value of 29.38 V. This case also showed the largest voltage variation during the steady-state interval, where the waveform repeatedly decreased to a lower voltage level between successive charging periods. When the capacitance was increased to 1000 µF, the average DC-link voltage increased to 30.45 V. This represents an increase of 1.07 V compared with the 470 µF case. The voltage waveform also showed a smaller voltage drop during each ripple cycle.

The 2200 µF capacitor further increased the average DC-link voltage to 31.03 V. Compared with the 1000 µF case, the increase was 0.58 V. The waveform remained closer to the upper voltage level for a longer period, indicating improved voltage retention during the intervals between rectifier charging peaks. The highest average DC-link voltage was obtained with the 22000 µF capacitor, reaching 31.25 V. However, the difference between the 2200 µF and 22000 µF cases was only 0.22 V. This result shows that, although a very large capacitance provides the highest average DC-link voltage, the additional increase in average voltage becomes relatively small at high capacitance values.

Overall, the average DC-link voltage increased from 29.38 V at 470 µF to 31.25 V at 22000 µF, corresponding to a total increase of 1.87 V. The results indicate that increasing the DC-link capacitance improves the voltage-holding capability of the rectifier output. Nevertheless, the improvement at higher capacitance values is more clearly reflected in the reduction of voltage ripple than in the increase of the average DC-link voltage.

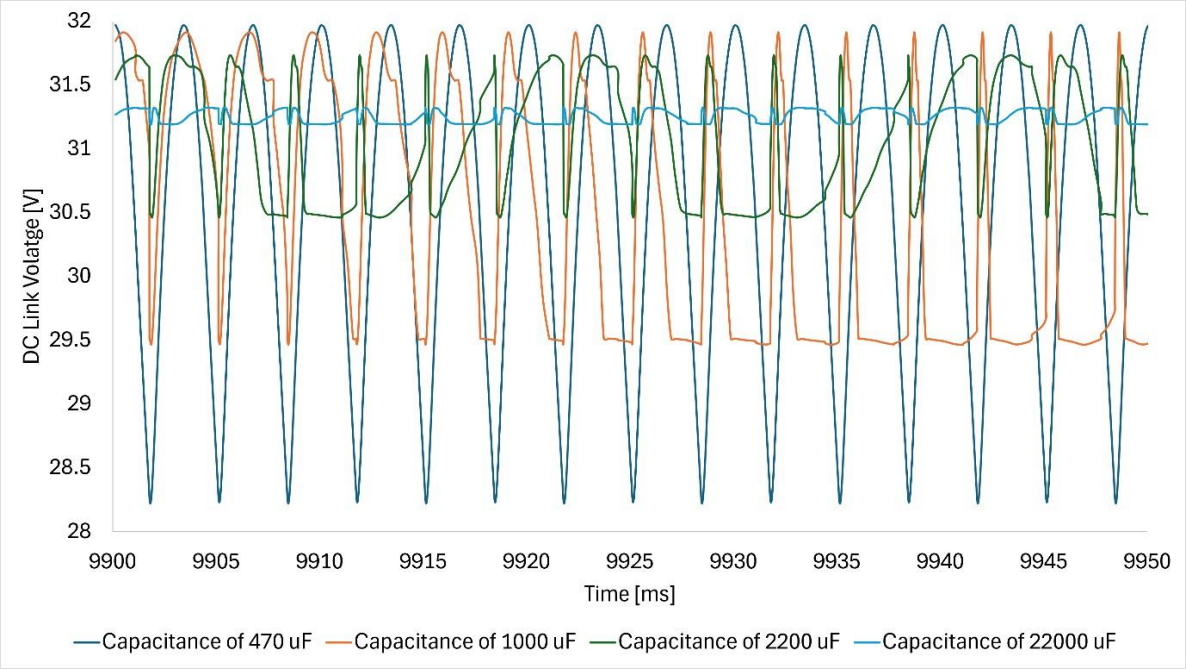

Figure 4. Steady-state DC-link voltage waveforms for different DC-link capacitance values from 9.90 s to 9.95 s

TABLE 5. AVERAGE DC-LINK VOLTAGE FOR DIFFERENT DC-LINK CAPACITANCE VALUES

Steady State Start [s]	Average DC Link Voltage [V]
9.9	29.38
9.9	30.45
9.9	31.03
9.9	31.25

3.4 Load power delivery

Figure 5 shows the load power waveforms during the steady-state interval from 9.90 s to 9.95 s for the four DC-link capacitance values. The corresponding average load current, average load power, maximum load power, minimum load power, and power fluctuation are summarized in Table 6.

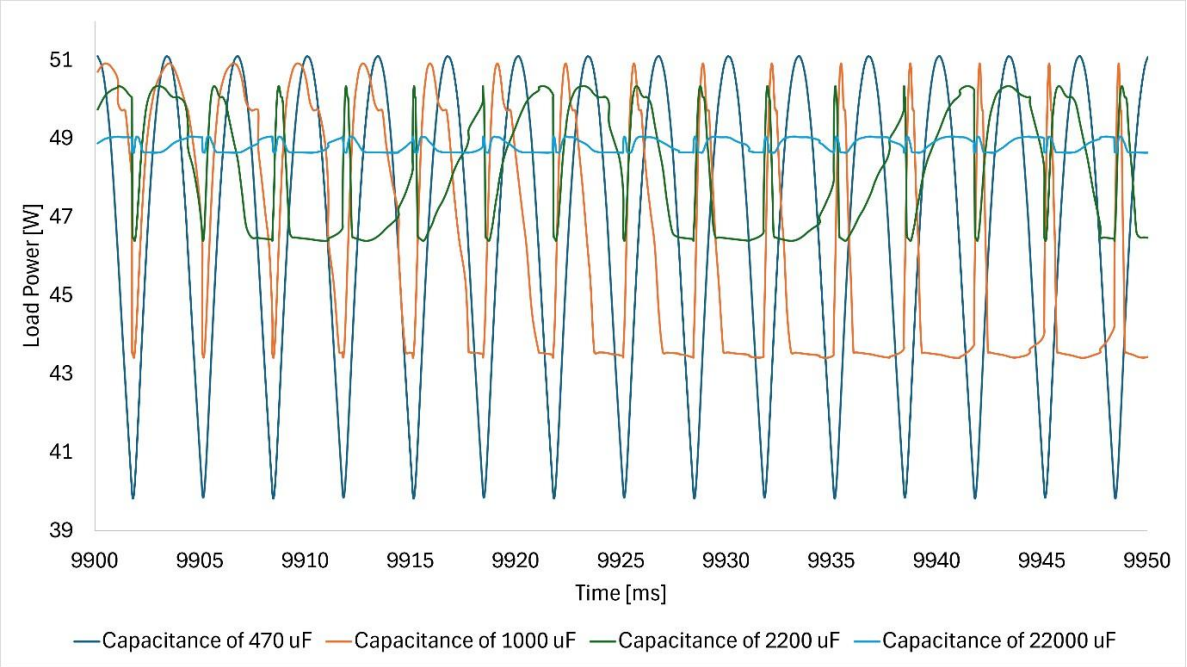

Figure 5. Steady-state load power waveforms for different DC-link capacitance values

TABLE 6. LOAD CURRENT AND POWER DELIVERY CHARACTERISTICS FOR DIFFERENT DC-LINK CAPACITANCE VALUES

Average Load Current [A]	Average Load Power [W]	Maximum Load Power [W]	Minimum Load Power [W]	Power Fluctuation [%]
1.47	43.25	51.11	39.83	11.28
1.52	46.41	50.92	43.41	7.51
1.55	48.14	50.35	46.40	3.95
1.56	48.83	49.05	48.64	0.41

The 470 µF case produced the lowest average load current and average load power, with values of 1.47 A and 43.25 W, respectively. This case also exhibited the largest power fluctuation. The load power varied from 39.83 W to 51.11 W, resulting in a peak-to-peak power fluctuation of 11.28 W. When the DC-link capacitance was increased to 1000 µF, the average load current increased to 1.52 A and the average load power increased to 46.41 W. The minimum load power increased to 43.41 W, while the power fluctuation decreased to 7.51 W.

The 2200 µF case further improved the power delivery characteristics. The average load current and average load power increased to 1.55 A and 48.14 W, respectively. The load power ranged from 46.40 W to 50.35 W, resulting in a power fluctuation of 3.95 W. The 22000 µF case produced the most stable load power waveform. The average load current reached 1.56 A, while the average load power reached 48.83 W. The maximum and minimum load powers were 49.05 W and 48.64 W, respectively, resulting in a power fluctuation of only 0.41 W.

Overall, increasing the DC-link capacitance improved both the average power delivered to the load and the stability of the delivered power. The average load power increased from 43.25 W at 470 µF to 48.83 W at 22000 µF, corresponding to an increase of 5.58 W. At the same time, the peak-to-peak power fluctuation decreased from 11.28 W to 0.41 W, representing a reduction of approximately 96.4%. These results are consistent with the DC-link voltage analysis. A lower voltage ripple resulted in a smaller variation in load current and load power. Although the 22000 µF capacitor provided the most stable power delivery, the difference in average load power between the 2200 µF and 22000 µF cases was relatively small, increasing from 48.14 W to 48.83 W. Therefore, the main benefit of the largest capacitance was the substantial reduction in power fluctuation rather than a large increase in average load power.

4. CONCLUSION

This study evaluated the effects of DC-link capacitance on output voltage quality and load power delivery in a three-phase diode rectifier circuit. Four capacitance values of 470 µF, 1000 µF, 2200 µF, and 22000 µF were compared under identical source and load conditions. The results showed that increasing the DC-link capacitance improved the steady-state voltage quality. The peak-to-peak DC-link voltage ripple decreased from 3.75 V at 470 µF to 0.13 V at 22000 µF, while the ripple percentage decreased from 12.75% to 0.42%. At the same time, the average DC-link voltage increased from 29.39 V to 31.25 V. The load power results showed a similar trend. The average load power increased from 43.25 W to 48.83 W, while the peak-to-peak power fluctuation decreased from 11.28 W to 0.41 W. Therefore, the principal benefit of increasing DC-link capacitance was the improvement of voltage and power stability rather than a substantial increase in average output voltage or average load power. Among the evaluated cases, the 22000 µF capacitor provided the best voltage quality and the most stable power delivery. However, the improvement in average DC-link voltage and average load power from 2200 µF to 22000 µF was relatively small. Therefore, the 2200 µF case may provide a practical compromise between voltage-ripple reduction, power-delivery stability, and capacitor size. Future work may include the analysis of capacitor ESR, source impedance, inrush current, non-resistive loads, and experimental validation of the simulation results.

5. ACKNOWLEDGEMENT

Not applicable.

6. REFERENCES

[1] J. Iwaszkiewicz, P. Mysiak, and A. Muc, "Current Controlled AC/DC Converter and Its Performance—A Mathematical Model," Energies, vol. 18, no. 2, p. 419, Jan. 2025, doi: 10.3390/en18020419.

[2] J.-Y. Lee, K.-W. Heo, K.-T. Kim, and J.-H. Jung, "Analysis and Design of Three-Phase Buck Rectifier Employing UPS to Supply High Reliable DC Power," Energies, vol. 13, no. 7, p. 1704, Jan. 2020, doi: 10.3390/en13071704.

[3] H. Ertl and J. W. Kolar, "A constant output current three-phase diode bridge rectifier employing a novel 'Electronic Smoothing Inductor,'" IEEE Transactions on Industrial Electronics, vol. 52, no. 2, pp. 454–461, Apr. 2005, doi: 10.1109/TIE.2005.843910.

[4] S. Li, L. Yang, and T. Wang, "Analysis of the DC-Link Voltage Ripple for the Three-Phase Voltage Source Converter under Nonlinear Output Current," Energies, vol. 15, no. 8, p. 2892, Jan. 2022, doi: 10.3390/en15082892.

[5] K. Uddin, A. D. Moore, A. Barai, and J. Marco, "The effects of high frequency current ripple on electric vehicle battery performance," Applied Energy, vol. 178, pp. 142–154, Sep. 2016, doi: 10.1016/j.apenergy.2016.06.033.

[6] M. A. Islam, K. N. Hasan, G. Lamb, and M. Datta, "Energy storage functions and technological developments of vehicle-to-everything enabled electric vehicle chargers: Converter designs, control strategies, services, and market readiness," Journal of Energy Storage, vol. 159, p. 121778, May 2026, doi: 10.1016/j.est.2026.121778.

[7] B. Wang and H. Tang, "An Analytical Model for DC-Link Capacitor Ripple Current in Multi-Phase H-Bridge Inverters," Processes, vol. 14, no. 7, p. 1059, Jan. 2026, doi: 10.3390/pr14071059.

[8] J. Fang, Q. Xu, Y. Xia, and L. Fang, "Research on super-capacitor fast power control system," Energy Reports, vol. 8, pp. 710–717, Apr. 2022, doi: 10.1016/j.egyr.2021.11.192.

[9] M. E. Meral and D. Çelik, "Mitigation of DC-link voltage oscillations to reduce size of DC-side capacitor and improve lifetime of power converter," Electric Power Systems Research, vol. 194, p. 107048, May 2021, doi: 10.1016/j.epsr.2021.107048.

[10] A. Carloni, F. Baronti, R. Di Rienzo, R. Roncella, and R. Saletti, "On the Sizing of the DC-Link Capacitor to Increase the Power Transfer in a Series-Series Inductive Resonant Wireless Charging Station," Energies, vol. 14, no. 3, p. 743, Jan. 2021, doi: 10.3390/en14030743.

[11] S. Banerjee, B. Mordina, P. Sinha, and K. K. Kar, "Recent advancement of supercapacitors: A current era of supercapacitor devices through the development of electrical double layer, pseudo and their hybrid supercapacitor electrodes," Journal of Energy Storage, vol. 108, p. 115075, Feb. 2025, doi: 10.1016/j.est.2024.115075.

[12] W. Liu et al., "Review of Energy Storage Capacitor Technology," Batteries, vol. 10, no. 8, p. 271, Aug. 2024, doi: 10.3390/batteries10080271.

[13] R. Thekkeppat, S. K. Singh, M. Lad, S. Bhongade, and P. Shrivastava, "Design and development of a rapid, high voltage capacitor charging power supply based on third order resonant converter topology," Rev. Sci. Instrum., vol. 92, no. 11, p. 114710, Nov. 2021, doi: 10.1063/5.0064900.

[14] J. Dang, F. Yang, Y. Li, X. Deng, and M. Ouyang, "Transient behaviors and mathematical model of proton exchange membrane electrolyzer," Journal of Power Sources, vol. 542, p. 231757, Sep. 2022, doi: 10.1016/j.jpowsour.2022.231757.

[15] A. Hassan, J. Ahmed, S. Papadopoulos, F. Kahwash, and K. Goh, "A comprehensive review of frequency response and control strategies for grid-connected solar photovoltaic systems," Renewable and Sustainable Energy Reviews, vol. 226, p. 116324, Jan. 2026, doi: 10.1016/j.rser.2025.116324.

[16] M. Jami, Q. Shafiee, M. Gholami, and H. Bevrani, "Control of a super-capacitor energy storage system to mimic inertia and transient response improvement of a direct current micro-grid," Journal of Energy Storage, vol. 32, p. 101788, Dec. 2020, doi: 10.1016/j.est.2020.101788.

[17] I. AL-Wesabi, A. A. Al-Shamma'a, H. M. Hussein Farh, R. A. Dawood, G. C. Mwakipunda, and J. Xu, "Capacitance estimation algorithm based on DC-link voltage ripples using hybrid machine learning techniques in power electronics converters," Results in Engineering, vol. 27, p. 106216, Sep. 2025, doi: 10.1016/j.rineng.2025.106216.

[18] A. Sarwar and M. S. J. Asghar, "Simulation and Analysis of a Multilevel Converter Topology for Solar PV Based Grid Connected Inverter," Smart Grid and Renewable Energy, vol. 2, no. 1, pp. 56–62, Feb. 2011, doi: 10.4236/sgre.2011.21007.

[19] E. N. Irawan, K.-I. Yamashita, and G. Fujita, "Adaptive Maximum Power Point Tracking for Optimizing Power Extraction in Small-Scale Wind Energy Systems," in 2025 60th International Universities Power Engineering Conference (UPEC), Sep. 2025, pp. 1–6. doi: 10.1109/UPEC65436.2025.11279821.

[20] M. S. Anindya, F. Zaro, and M. Popescu, “Power Quality Improvement Using Active Power Filters in Industrial Systems,” RESWARA: Jurnal Riset Ilmu Teknik, vol. 3, no. 2, pp. 44–50, Apr. 2025, doi: 10.70716/reswara.v3i2.404.

[21] T. Mishima, “Essential and Core Technologies for High-Frequency Switch-mode Power Converters-Introduction-,” The Journal of The Institute of Electrical Engineers of Japan, vol. 143, no. 1, pp. 9–12, 2023, doi: 10.1541/ieejjournal.143.9.

[22] R. A.a., S. Paulose, M. Thomas, and J. Joy, “PWM control strategies for Switched-Capacitor inverters,” Materials Today: Proceedings, vol. 58, pp. 516–522, Jan. 2022, doi: 10.1016/j.matpr.2022.03.049.

[23] B. Sharma, S. Manna, V. Saxena, P. K. Raghuvanshi, M. H. Alsharif, and M.-K. Kim, “A comprehensive review of multi-level inverters, modulation, and control for grid-interfaced solar PV systems,” Sci Rep, vol. 15, no. 1, p. 661, Jan. 2025, doi: 10.1038/s41598-024-84296-1.